Physical Communication 1 (2008) 221–228

Contents lists available at ScienceDirect

Physical Communication

journal homepage: www.elsevier.com/locate/phycom

Full length article

Reduced-complexity cluster modeling for time-variant wideband MIMO channels

Hui Xiao, Alister G. Burr *

Department of Electronics, University of York, York, YO10 5DD, United Kingdom

ARTICLE INFO

Keywords:
MIMO
Time-variant
Wideband
Cluster
Channel modeling
Reduced-complexity

ABSTRACT

This paper presents a reduced-complexity cluster modeling method for channel models that are based on the 3GPP and similar channel models to simulate the time variation of spatially correlated wideband MIMO channels. The main novelty is that, when modeling the time-variant wideband MIMO channels, instead of tracking the changes in the angles of arrival (AoAs) of all the multi-path components (MPCs) defined, we only track the change in the centre AoA for each of the clusters. Hence for moderate angle spreads (ASs) of clusters and a constant uniform distribution of the offsets of the MPCs within each cluster, tracking the time-variant centre AoAs of the clusters allows us to develop a computationally efficient approximation method to calculate the instantaneous channel matrix and spatial correlation matrix for time-variant wideband MIMO channels. The development of this approximation method includes two stages: firstly, we evaluate the approximation method for simulating wideband MIMO channels with time-invariant AoAs in terms of the centre angles and scatterer distributions of clusters; secondly, on the basis of the validation at stage one, we develop the approximation method for the wideband MIMO channels with time-variant AoAs, and evaluate this approximation method by the extended correlation matrix distance (CMD) metric. We use the extended CMD metric to compare the CMDs predicted by the approximate and exact calculation under different time-variant scenarios. The simulation results show that the approximation method works well when the velocity of the movement is up to 50 m/s and provided the ASs of the clusters are within 10°.
© 2008 Elsevier B.V. All rights reserved.

1. Introduction

The technology of using multiple antennas at both link ends in wireless communications systems, known as MIMO, has been introduced as an effective way to meet user demand for high data rate applications [12–14]. The efficiency of MIMO technology directly depends on the propagation environment between the transmitter (*Tx*) and the receiver (*Rx*), i.e. the MIMO channel. In reality, there exist time variation, frequency selectiveness, and spatial correlation in MIMO transmission channels, which influence the realistic performance of MIMO systems. For example, some research in this field show that significant spatial correlation of MIMO channels, which is due to the uneven distribution of the scatterers in the propagation environment, generally has an adverse effect on capacity and error rate performance [1], and it has been shown in [2] that channel models disregarding clustering effects overestimate channel capacity. Thus, simulating realistic MIMO channels is essential to predict the performance of real MIMO systems.

In our previous work presented in [3], we built up a geometry-based stochastic (GBS) MIMO channel model [4–6] based on the Third Generation Partnership Project (3GPP) spatial channel model (SCM) [4] to realistically simulate the short-term time variation of the spatially correlated wideband MIMO channels which we named the newly extended 3GPP SCM (NE-3GPP SCM). The main advantage of the NE-3GPP SCM is that it can mimic the time

* Corresponding author.
E-mail addresses: hx501@ohm.york.ac.uk (H. Xiao), alister@ohm.york.ac.uk (A.G. Burr).

1874-4907/$ – see front matter © 2008 Elsevier B.V. All rights reserved.
doi:10.1016/j.phycom.2008.07.002

variation of spatially correlated wideband MIMO channels in outdoor scenarios more accurately and is more comparable to real measurements, based on the consideration of some further time-variant channel parameters that are important to modeling the time-variant characteristics of wideband MIMO channels but can be easily calculated without adding too much complexity to the modeling.

However, since the NE-3GPP SCM is based on the 3GPP SCM, which is one of the GBS channel models that adopts the concept of scattering clusters (referred to in the 3GPP document [4] as "paths") containing a number of stochastically varying multi-path components (MPCs) ("sub-paths" in the 3GPP terminology), it requires defined directions and complex path gains for all MPCs to generate each channel realization, which can result in considerable implementation complexity in system simulation for large networks. Based on our further studies in this area, we found that the steering vectors for uniform linear arrays (ULAs) can be approximated by the Taylor series expansion approach, and that for moderate angle spreads (ASs) the approximated steering vectors allow us to deduce a closed-form approximation to the spatial channel correlation matrix for MIMO channels which depends only on the moments of the scatterer distributions. This enables us to simulate the spatial correlation matrix of MIMO channels on a cluster-by-cluster basis with each cluster modeled by a few terms instead of using the full number of MPCs. Since the calculation of the channel matrix of a MIMO system can be deduced directly from the spatial correlation matrix of the MIMO channels, the computational efficiency introduced by the approximate calculation of the spatial correlation matrix has direct influence on the complexity reduction in the calculation of the channel matrix. We evaluate this approximation method for wideband MIMO channels with time-invariant angles of arrival (AoAs) by the mean square error (MSE) metric and capacity metric, respectively. The simulation results show that, when the AoAs are time-invariant, the approximation method works well for clusters with uniform distribution of the angle offsets of the MPCs within each cluster and AS of each cluster within 15°.

Therefore, we propose a practical alternative to the exact calculation suggested by the 3GPP SCM to simulate the spatial correlation matrix and the channel matrix for time-variant wideband MIMO channels, with much lower computational complexity. The time-variant wideband channels are simulated by tracking the changes in the time-variant AoAs of all the MPCs using the method suggested by the NE-3GPP SCM [3], based on a practical assumption that the time variation of channels is only due to the movement of the *Rx*. The main novelty of our work is that, when modeling the time-variant wideband MIMO channels, instead of tracking the changes in the AoAs of all the MPCs defined, we track the time variation of MIMO channels cluster-by-cluster, and only track the change in the centre AoA for each of the clusters. Thus, for moderate ASs of clusters and constant uniform distribution of the offsets of the MPCs within each cluster, knowing the time-variant centre AoAs of the clusters, we can use the reduced-complexity cluster modeling method to simulate the time-variant wideband MIMO channels with much lower computational complexity. The validity, reliability and accuracy of the proposed method are evaluated using the extended correlation matrix distance (CMD) metric [8]. The comparisons of the CMDs predicted by the proposed approximation method and the exact calculation are carried out in various time-variant scenarios with different velocities of the movement. The simulation results show that the proposed approximation method can model the time variation of wideband MIMO channels with acceptable accuracy and low complexity, when the velocity of the movement up is to 50 m/s and provided the ASs of the clusters are within 10°.

The rest of the paper is organized as follows: the exact calculation of the channel matrix and spatial correlation matrix for time-variant wideband MIMO channels are introduced in Section 2. Section 3 presents the approximation method in detail. The evaluation of this approximation method for the wideband MIMO channels with time-invariant AoAs using the MSE and capacity metric, and for those channels with time-variant AoAs using the extended CMD metric are shown in Section 4. Finally, conclusions drawn from the simulation results are given in Section 5.

In this paper, the following notations are defined as: the symbol $(\cdot)^{\mathrm{T}}$ means matrix transposition; $(\cdot)^*$ stands for complex conjugation; $(\cdot)^{\mathrm{H}}$ stands for matrix Hermitian; $\overline{(\cdot)}$ denotes the expectation; $\|\cdot\|_2$ is the Frobenius norm of the given matrix; $\delta(\cdot)$ is the Dirac delta function; vec $(\cdot)$ is to vectorize a given matrix: that is, to form a vector by stacking the columns of the matrix.

2. Exact calculations of the channel matrix and spatial correlation matrix for time-variant wideband MIMO channels

The time-variant wideband MIMO channels are simulated based on the 3GPP SCM. Fig. 1 shows the geometry of the parameters in the 3GPP SCM. In the 3GPP SCM, there are a fixed number (6) of spatially separated "paths" with different time delays of arrival (TDoAs) in every scenario, each of the paths being made up of 20 spatially separated MPCs. Here we use N to denote the total number of "paths", which correspond to clusters in this paper, and M to stand for the number of MPCs ("sub-paths" in 3GPP) in each path. In order to characterize the time dispersion of the wideband channels, the time-variant channel matrix for the channels with n_T *Tx* antennas and n_R *Rx* antennas is defined for each of the paths with different TDoAs as follows:

$$\mathbf{H}(t,\tau_n) = \boldsymbol{\Psi}_{R,n}\boldsymbol{\Xi}_n\boldsymbol{\Psi}_{T,n}^{\mathrm{T}} = \sum_{p=A}^{B}\delta\left(\tau_n-\tau_p\right) \times \xi_p\boldsymbol{\Phi}_R\left(\theta_{R,p}(t)\right)\boldsymbol{\Phi}_T^{\mathrm{T}}\left(\theta_{T,p}(t)\right) \quad (1)$$

where $n = 1\dots N, A = (n-1)M+1, B = (n-1)M+M$ and $\mathbf{H}(t,\tau_n)$ denote the $n_R \times n_T$ channel matrix for the nth path which arrives at the *Rx* with TDoA τ_n. The matrices $\boldsymbol{\Psi}_{R,n}$ and $\boldsymbol{\Psi}_{T,n}$ denote the steering vector matrices at the *Rx* side and the *Tx* side, respectively, of dimension $n_R \times M$ and $n_T \times M$, respectively. Their columns are the vectors $\boldsymbol{\Phi}_R\left(\theta_{R,p}(t)\right)$ and $\boldsymbol{\Phi}_T\left(\theta_{T,p}(t)\right)$, respectively. In this paper,

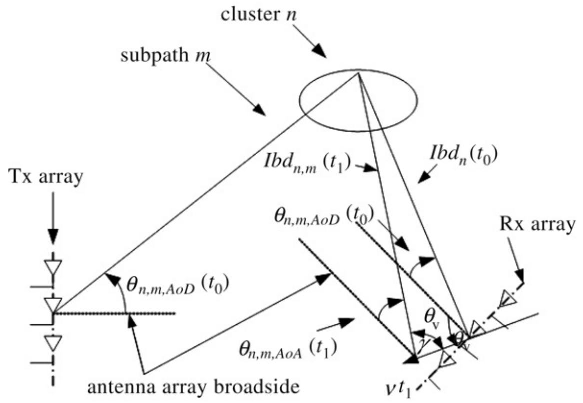

Fig. 1. Geometry of the parameters in the cluster-based 3GPP SCM.

a ULA is used for both the *Tx* and the *Rx* side. $\theta_{R,p}(t)$ and $\theta_{T,p}(t)$ stand for the AoA and angle of departure (AoD) for the pth sub-path within the nth path, respectively. Since we assume the time variation is only due to the movement of the *Rx* in this paper, $\theta_{T,p}(t)$ is taken as constant, so we omit the argument t in it. The time variation of the AoAs are tracked using the method suggested by the NE-3GPP SCM, so the detailed procedures for the calculation of the time-variant AoAs are given in the Appendix A, and the parameters needed in the calculation are shown in Fig. 1. The matrix $\boldsymbol{\Xi}_n$ is an $M \times M$ matrix diagonal matrix containing the complex path gains of the sub-paths within a path, with diagonal elements ξ_p.

Now we rewrite Eq. (1) as:

$$\mathbf{H}(t,\tau_n) = \sum_{p=A}^{B} \delta\left(\tau_n - \tau_p\right) \xi_p \boldsymbol{\Phi}_R\left(\theta_{R,p}(t)\right) \boldsymbol{\Phi}_T^{\mathrm{T}}\left(\theta_{T,p}\right). \qquad (2)$$

The definitions of $\boldsymbol{\Phi}_R\left(\theta_{R,p}(t)\right)$, $\boldsymbol{\Phi}_T^{\mathrm{T}}\left(\theta_{T,p}\right)$ and ξ_p are as follows [9]:

$$\boldsymbol{\Phi}_R\left(\theta_{R,P}(t)\right) = \left\{\exp\left(j2\pi \frac{il_R}{\lambda} \sin(\theta_{R,P}(t))\right), i = 1 \dots n_R\right\} \qquad (3)$$

$$\boldsymbol{\Phi}_T(\theta_{T,P}) = \left\{\exp\left(j2\pi \frac{kl_T}{\lambda} \sin(\theta_{T,P})\right), k = 1 \dots n_T\right\} \qquad (4)$$

where λ is the wavelength of the radio wave, l_R and l_T denote the antenna intervals in the ULA at the *Rx* side and *Tx* side, respectively. The variables i and k are used to denote the positions of the antenna elements in the *Rx* and *Tx* antenna array, respectively.

$$\xi_p = \sqrt{P_p}\sqrt{G_{Tx}\left(\theta_{T,P}\right)}\sqrt{G_{Rx}}e^{j\phi_p} \qquad (5)$$

where P_p stands for the power of the pth sub-path within the nth path, $G_{Tx}\left(\theta_{T,p}\right)$ and G_{Rx} are the antenna gains of the *Tx* antenna and *Rx* antenna, respectively, for the pth sub-path within the nth path, since the *Rx* antenna pattern in the 3GPP SCM is omni-directional with an antenna gain of −1 dBi, the argument $\theta_{R,p}(t)$ in G_{Rx} is neglected here. ϕ_p denotes the phase of the pth component arriving at the *Rx*.

Based on the definition of the exact calculation of the time-variant channel matrix for the wideband MIMO channels, the channel realization between the ath *Rx* antenna and the bth *Tx* antenna based on the nth cluster is calculated as:

$$h_{ab}(t,\tau_n) = \sum_{p=A}^{B} \delta\left(\tau_n - \tau_p\right) \xi_p \Psi_{R,a}\left(\theta_{R,p}(t)\right) \Psi_{T,b}\left(\theta_{T,p}\right) \qquad (6)$$

where $\Psi_{R,a}\left(\theta_{R,p}(t)\right)$ and $\Psi_{T,b}\left(\theta_{T,p}\right)$ are the steering values related to the pth sub-path within the cluster at the ath *Rx* antenna and the bth *Tx* antenna, respectively, $a = 1 \dots n_R$, $b = 1 \dots n_T$, $n = 1 \dots N$.

Thus, the instantaneous spatial correlation [9] between the (a, b)th channel h_{ab}, and the (c, d)th channel h_{cd} is defined as:

$$\begin{aligned} R_{ab,cd}(t,\tau_n) &= \overline{h_{ab}(t,\tau_n)\, h_{cd}^{*}(t,\tau_n)} \\ &= \overline{\sum_{p=A}^{B} \xi_p \Psi_{R,a}\left(\theta_{R,p}(t)\right) \Psi_{T,b}\left(\theta_{T,p}\right) \left(\sum_{q=A}^{B} \xi_q \Psi_{R,c}\left(\theta_{R,q}(t)\right) \Psi_{T,d}\left(\theta_{T,q}\right)\right)^{*}} \end{aligned} \qquad (7)$$

where $a, c = 1 \dots n_R$ and $b, d = 1 \dots n_T$. In this paper, to generate the instantaneous spatial correlation between two MIMO channels, the expectation is taken over an ensemble of multi-path phases, and the phases in (5) for all the components in a specific cluster are drawn from a uniform random distribution on 0°–360°. Thus, the complex path gains of the MPCs are independent from each other, that is the individual MPCs in a cluster are subject to independent fading. Therefore, $\overline{\xi_p \xi_q^*} = 0$, if $p \neq q$, and hence (7) can be further simplified as:

$$\begin{aligned} R_{ab,cd}(t,\tau_n) &= \sum_{p=A}^{B} \overline{\left|\xi_p\right|^2 \Psi_{R,a}\left(\theta_{R,p}(t)\right) \Psi_{T,b}\left(\theta_{T,p}\right) \Psi_{R,c}^{*}\left(\theta_{R,p}(t)\right) \Psi_{T,d}^{*}\left(\theta_{T,p}\right)} \\ &= \sum_{p=A}^{B} \overline{\left|\xi_p\right|^2} \Psi_{R,a}\left(\theta_{R,p}(t)\right) \Psi_{T,b}\left(\theta_{T,p}\right) \Psi_{R,c}^{*}\left(\theta_{R,p}(t)\right) \Psi_{T,d}^{*}\left(\theta_{T,p}\right). \end{aligned} \qquad (8)$$

3. The approximation method to simulate time-variant wideband MIMO channels

3.1. Introduction to the reduced-complexity cluster modeling method for MIMO channels with time-invariant angles of arrival

Here we introduce the reduced-complexity cluster modeling method for wideband MIMO channels with time-invariant AoAs. Fig. 2 is a demonstration of the cluster-based calculation.

If the AS of the cluster is moderate, then the Taylor series expansion [10] can be applied to the steering vector functions (3) and (4) to approximate the steering values with respect to the centre angle of the cluster. Thus, we can calculate $\Psi_{R,a}\left(\theta_{R,p}\right)$ as:

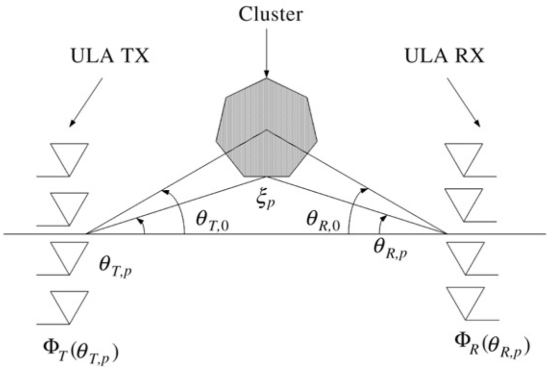

Fig. 2. Demonstration of the cluster-based calculation.

$$\Psi_{R,a}\left(\theta_{R,p}\right) = \Psi_{R,a}(\theta_{R,0}) + \Psi'_{R,a}(\theta_{R,0})(\theta_{R,P}-\theta_{R,o}) + \frac{\Psi''_{R,a}\left(\theta_{R,0}\right)}{2!}(\theta_{R,P}-\theta_{R,0})^2 + \frac{\Psi'''_{R,a}\left(\theta_{R,0}\right)}{3!}(\theta_{R,P}-\theta_{R,0})^3 + \cdots \tag{9}$$

where $\theta_{R,0}$ stands for the centre AoA of the cluster, $\Psi'_{R,a}\left(\theta_{R,0}\right)$, $\Psi''_{R,a}\left(\theta_{R,0}\right)$ and $\Psi'''_{R,a}\left(\theta_{R,0}\right)$ are the first, second and third order differentials of $\Psi_{R,a}\left(\theta_{R,p}\right)$ at $\theta_{R,0}$. Then we substitute (3) for the terms in (9), which will lead (9) to a power series form:

$$\Psi_{R,a}\left(\theta_{R,p}\right) = \Psi_{R,a}(\theta_{R,0})\left(1+\alpha_{1,a}(\theta_{R,0})(\theta_{R,P}-\theta_{R,0}) + \alpha_{2,a}(\theta_{R,0})(\theta_{R,P}-\theta_{R,0})^2 + \cdots\right) \tag{10}$$

where the detailed forms of $\alpha_{1,a}\left(\theta_{R,0}\right)$, $\alpha_{2,a}\left(\theta_{R,0}\right)\ldots$ are calculated by MAPLE [11], assuming $\lambda/2$ antenna element spacing. Please refer to Appendix B for the detailed forms of these coefficients. Similarly the terms $\Psi_{T,b}\left(\theta_{T,p}\right)$, $\Psi^*_{R,c}\left(\theta_{R,p}\right)$ and $\Psi^*_{T,d}\left(\theta_{T,p}\right)$ in (8) can also be expressed in power series form, thus we can deduce the closed-form approximate calculation of $R_{ab,cd}(\tau_n)$ by using the first six polynomial terms truncated from the full expression of the approximate spatial correlation $\hat{R}_{ab,cd}(\tau_n)$. So the approximate calculation of $R_{ab,cd}(\tau_n)$ is defined as:

$$\hat{R}_{ab,cd}(\tau_n) = \Psi_{R,a}\left(\theta_{R,0}\right)\ldots\Psi^*_{T,d}\left(\theta_{T,0}\right) \times \begin{pmatrix} \sum_{p=A}^{B}\overline{\left|\xi_p\right|^2} + A_{10}\left(\theta_{R,0}\right)\sum_{p=A}^{B}\overline{\left|\xi_p\right|^2}\left(\Delta\theta_{R,p}\right) \\ +A_{01}\left(\theta_{T,0}\right)\sum_{p=A}^{B}\overline{\left|\xi_p\right|^2}\left(\Delta\theta_{T,p}\right) \\ +A_{20}\left(\theta_{R,0}\right)\sum_{p=A}^{B}\overline{\left|\xi_p\right|^2}\left(\Delta\theta_{R,p}\right)^2 \\ +A_{02}\left(\theta_{T,0}\right)\sum_{p=A}^{B}\overline{\left|\xi_p\right|^2}\left(\Delta\theta_{T,p}\right)^2 \\ +A_{11}\left(\theta_{R,0},\theta_{T,0}\right)\sum_{p=A}^{B}\overline{\left|\xi_p\right|^2}\left(\Delta\theta_{R,p}\right)\left(\Delta\theta_{T,p}\right)\ldots \end{pmatrix} \tag{11}$$

where $\Delta\theta_{R,p}$ and $\Delta\theta_{T,p}$ denote the offsets of the pth subpath with respect to the centre AoA and AoD individually, and coefficients $A_{10}\left(\theta_{R,0}\right), A_{01}\left(\theta_{T,0}\right)\ldots A_{11}\left(\theta_{R,0},\theta_{T,0}\right)$ are only functions of the centre angles of the cluster. Obviously, for the cluster with a moderate angle spread, the higher order used in the Taylor series expansion, the greater the total number of the polynomial terms will be in the calculation of $\hat{R}_{ab,cd}$, thus the value of $\hat{R}_{ab,cd}$ will be closer to that of $R_{ab,cd}$. However, the calculation of $\hat{R}_{ab,cd}$ with a large number of polynomial terms included in (11) will result in significant computational complexity. For example, with the second order Taylor series expansion, the total number of polynomial terms in (11) is 25; if the third order Taylor series expansion is used, the total number of polynomial terms in (11) will be 49; the fourth order Taylor series expansion can lead to 81 polynomial terms in total included in (11). Notice that whatever the order of the Taylor series expansion used is, the first six polynomial terms in (11) are the same, which are the constant, $A_{10}\left(\theta_{R,0}(t)\right)\sum_{p=A}^{B}\overline{\left|\xi_p\right|^2}\left(\Delta\theta_{R,p}\right)$, $A_{01}\left(\theta_{T,0}\right)\sum_{p=A}^{B}\overline{\left|\xi_p\right|^2}\left(\Delta\theta_{T,p}\right)$, $A_{20}\left(\theta_{R,0}(t)\right)\sum_{p=A}^{B}\overline{\left|\xi_p\right|^2}(\Delta\theta_{R,p})^2$, $A_{02}\left(\theta_{T,0}\right)\sum_{p=A}^{B}\overline{\left|\xi_p\right|^2}\left(\Delta\theta_{T,p}\right)^2$, $A_{11}\left(\theta_{R,0}(t),\theta_{T,0}\right)\sum_{p=A}^{B}\overline{\left|\xi_p\right|^2}\left(\Delta\theta_{R,p}\right)\left(\Delta\theta_{T,p}\right)$. Note that the summations in these terms are the product moments up to second order of the offset angles $\Delta\theta_T$, $\Delta\theta_R$. Therefore, we are interested in whether these six terms are sufficient to calculate $\hat{R}_{ab,cd}(\tau_n)$, and if so, in what angle spread range of the cluster the approximation method works well. The answers to these questions will be given in Section 4. For more details, refer to [7].

3.2. The approximation method for time-variant wideband MIMO channels

To develop the approximation method given in (11) for wideband MIMO channels with time-variant AoAs, we include the tracking of the change in the centre AoA for each cluster with time, and we assume a constant uniform (but not necessarily correlated) distribution of the offsets of the MPCs within each cluster. Therefore, the approximate calculation of $R_{ab,cd}(t)$ is defined by (12).

$$\hat{R}_{ab,cd}(t,\tau_n) = \Psi_{R,a}\left(\theta_{R,0}(t)\right)\ldots\Psi^*_{R,c}\left(\theta_{R,0}(t)\right)\Psi^*_{T,d}\left(\theta_{T,0}\right) \times \begin{pmatrix} \sum_{p=A}^{B}\overline{\left|\xi_p\right|^2} + A_{10}\left(\theta_{R,0}(t)\right)\sum_{p=A}^{B}\overline{\left|\xi_p\right|^2}\left(\Delta\theta_{R,p}\right) \\ +A_{01}\left(\theta_{T,0}\right)\sum_{p=A}^{B}\overline{\left|\xi_p\right|^2}\left(\Delta\theta_{T,p}\right) \\ +A_{20}\left(\theta_{R,0}(t)\right)\sum_{p=A}^{B}\overline{\left|\xi_p\right|^2}\left(\Delta\theta_{R,p}\right)^2 \\ +A_{02}\left(\theta_{T,0}\right)\sum_{p=A}^{B}\overline{\left|\xi_p\right|^2}\left(\Delta\theta_{T,p}\right)^2 \\ +A_{11}\left(\theta_{R,0}(t),\theta_{T,0}\right)\sum_{p=A}^{B}\overline{\left|\xi_p\right|^2}\left(\Delta\theta_{R,p}\right)\left(\Delta\theta_{T,p}\right) \end{pmatrix}. \tag{12}$$

According to the relationship between the full spatial correlation matrix and the channel matrix, using (12), we can generate $\hat{\mathbf{H}}(t,\tau_n)$ by:

$$\mathrm{vec}\left\{\hat{\mathbf{H}}(t,\tau_n)\right\} = \hat{\mathbf{R}}^{1/2}(t,\tau_n)\mathrm{vec}\{\mathbf{G}\}. \tag{13}$$

In (13), matrix $\mathbf{G}$ is an $n_R \times n_T$ matrix with all its entries being independently identically distributed (i.i.d.) complex Gaussian random values. A single independent instance of $\mathbf{H}$ can be obtained using a randomly chosen instance of $\mathbf{G}$; a time series of channel matrices, having a specific Doppler spectrum, can be generated from a time series of $\mathbf{G}$ matrices in which each element has the appropriate Doppler spectrum.

4. Evaluation of the approximation method

4.1. Validation of the approximation method using the mean square error metric

We use the mean square error (MSE) metric [15] to measure the performance degradations caused by the approximate calculation of the spatial correlation matrix in (11), as a function of the number of truncated polynomial terms used. Thus, we can evaluate if the six terms in (11) are sufficient to calculate $\hat{R}_{ab,cd}(\tau_n)$, and if so, in what angle spread range of the cluster the approximation method works well.

The spatial correlation matrix generated from the exact method suggested by the 3GPP channel model is taken as reference for the performance analysis, since this method does not use any approximation. The calculation of the MSE in units of dB is defined as:

$$\mathrm{MSE} = 10\log_{10}\left(\frac{\left\|\hat{\mathbf{R}} - \mathbf{R}\right\|_2}{\|\mathbf{R}\|_2}\right). \tag{14}$$

The simulation results of the MSE versus the number of the truncated polynomial terms in (11) are shown in Fig. 3.

In Fig. 3, line "a", "b" and "c" correspond to the second, third and fourth order Taylor series expansions used in (9), respectively. For each case, a set of MSEs is calculated for the corresponding approximation calculations plotted against the number of truncated polynomial terms as abscissa. Abscissa 1 means that only the constant term is used; abscissa 3 implies that the first three terms are used; abscissa 6 means that the first six terms are used, etc. In Fig. 3, from subfigures (a) to (c), the angle offsets of the cluster components are drawn from a uniform random distribution on $(-5\ -5)^\circ$, $(-7.5\ -7.5)^\circ$ and $(-10\ -10)^\circ$, respectively.

Fig. 3 shows that the MSE increases with angle spread, and, in general decreases with increasing number of terms included in the approximation (11) and with increasing order of the Taylor series. However for large angular spread and low order Taylor series the error increases with number of terms beyond 6 or 10 terms. This is because of the mismatch between the order of the Taylor series and the number of terms in total: the higher order terms are not accurate. However we note that for a 6 term approximation, compared to a single term the error is reduced by 30 dB for 10 degrees, 20 dB for 15 degrees, 15 dB for 20 degrees, which shows that the approximation with 6 terms is quite adequate for angle spread up to 15°.

This suggests that 6 terms give the optimum trade-off between accuracy and complexity. In the next part, we apply this approximation method to calculate the cumulative distribution function (CDF) of the capacity of MIMO channels, to validate its performance.

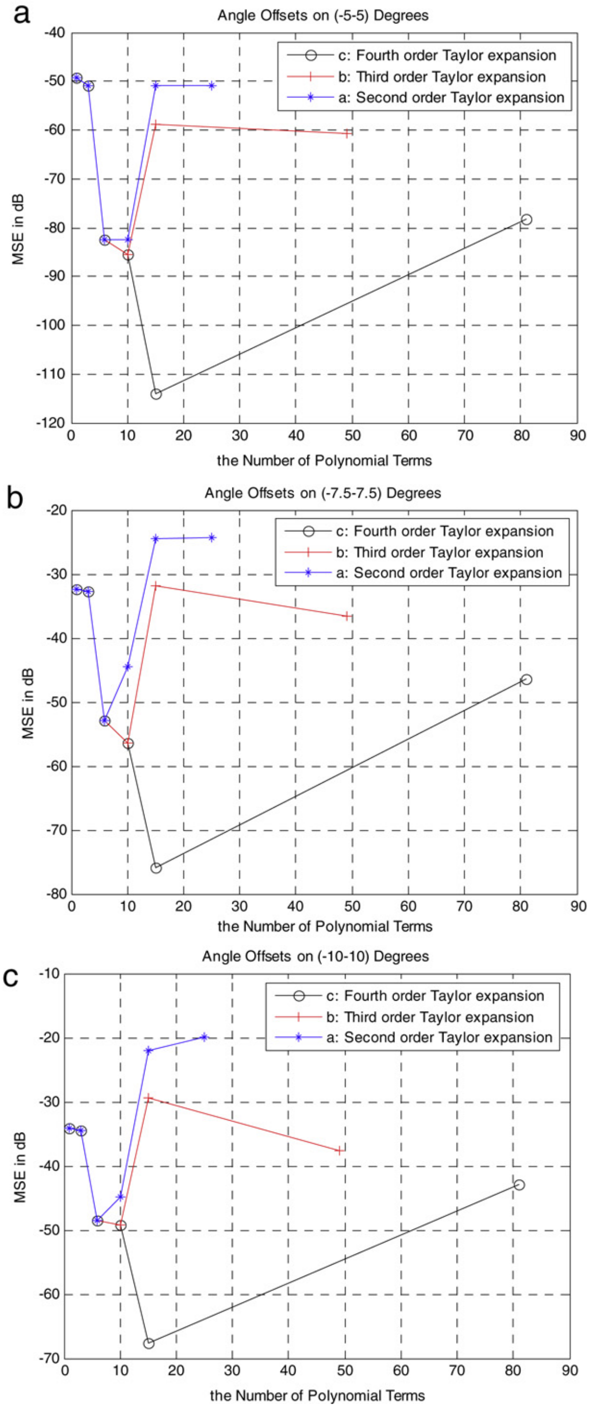

Fig. 3. The simulation results for the MSE.

4.2. The performance of the approximation method in calculating the CDF of the capacity of MIMO channels

The capacity of a MIMO channel is defined by the function below [13]:

$$C = W\log_2\det\left(\mathbf{I} + \frac{S}{N}\mathbf{H}\mathbf{H}^{\mathrm{H}}\right) \tag{15}$$

where S/N is the signal-to-noise ratio (SNR), and $\mathbf{I}$ is the identity matrix with dimensions $n_R \times n_R$, the bandwidth W is set to unit so that C denotes the bandwidth efficiency in units of bit/s/Hz. $\mathbf{HH}^{\mathrm{H}}$ is the channel correlation matrix at the receiver side, which we will calculate using (16).

$$
\begin{aligned}
R_{R_{i,i'}} &= \overline{\sum_{k=1}^{n_T}\sum_{p=A}^{B}\xi_p\Psi_{R,i}(\theta_{R,p})\Psi_{T,k}(\theta_{T,p})\left(\sum_{k'=1}^{n_T}\sum_{q=A}^{B}\xi_q^*\Psi_{R,i'}^*(\theta_{R,q})\Psi_{T,k'}^*(\theta_{T,q})\right)}\\
&= \sum_{k=1}^{n_T}\sum_{k'=1}^{n_T}\sum_{p=A}^{B}\overline{|\xi_p|^2\Psi_{R,i}(\theta_{R,p})\Psi_{T,k}(\theta_{T,p})\Psi_{R,i'}^*(\theta_{R,p})\Psi_{T,k'}^*(\theta_{T,p})}\\
&= \sum_{k=1}^{n_T}\sum_{k'=1}^{n_T}\sum_{p=A}^{B}\overline{|\xi_p|^2}\Psi_{R,i}(\theta_{R,p})\Psi_{T,k}(\theta_{T,p})\Psi_{R,i'}^*(\theta_{R,p})\Psi_{T,k'}^*(\theta_{T,p}) \qquad (16)
\end{aligned}
$$

where $R_{R_{i,i'}}$ stands for the channel correlation between a pair of Rx antennas i and i'. The simulations are for a MIMO system having two Tx and two Rx antennas, with antenna elements in the arrays $\lambda/2$ spaced apart. We compare the simulated CDFs of the capacity predicted by $\hat{R}_{R_{i,i'}}$ and $R_{R_{i,i'}}$, In Fig. 4, from subfigure (a) to (c), the simulated CDFs are depicted for angle spreads of 6°, 10° and 15°, respectively, and the SNR is 10 dB. For each case, the CDF deduced from $\hat{R}_{R_{i,i'}}$ is calculated in three ways to show the influence of the number of the truncated polynomial terms on the performance of the approximation calculation.

The simulation results show that in all these cases using the first six truncated polynomial terms in (11) can provide an estimate of the CDF of the capacity very close to the exact prediction. Although some error remains, the computational complexity has been greatly reduced from calculating all the MPCs one by one to simulating the cluster in terms of its centre angle and its angle spread. (Note also that the first two and the last of the 6 terms in (11) are typically very small, which may further reduce complexity). We find that, on the one hand, for the exact method, the channel realization for each cluster needs to calculate the product of several complex-valued exponentials for every MPC within a cluster, and then to add all the products up; on the other hand, by using the approximation method, for each cluster, we only need to calculate the complex-valued exponential multiplication for the centre angle, and the coefficients As once that only depend on the centre angle and are in terms of sin (·), cos (·) functions, and then by using the moments of the scatterer distribution together, we can simulate each cluster by six polynomial terms.

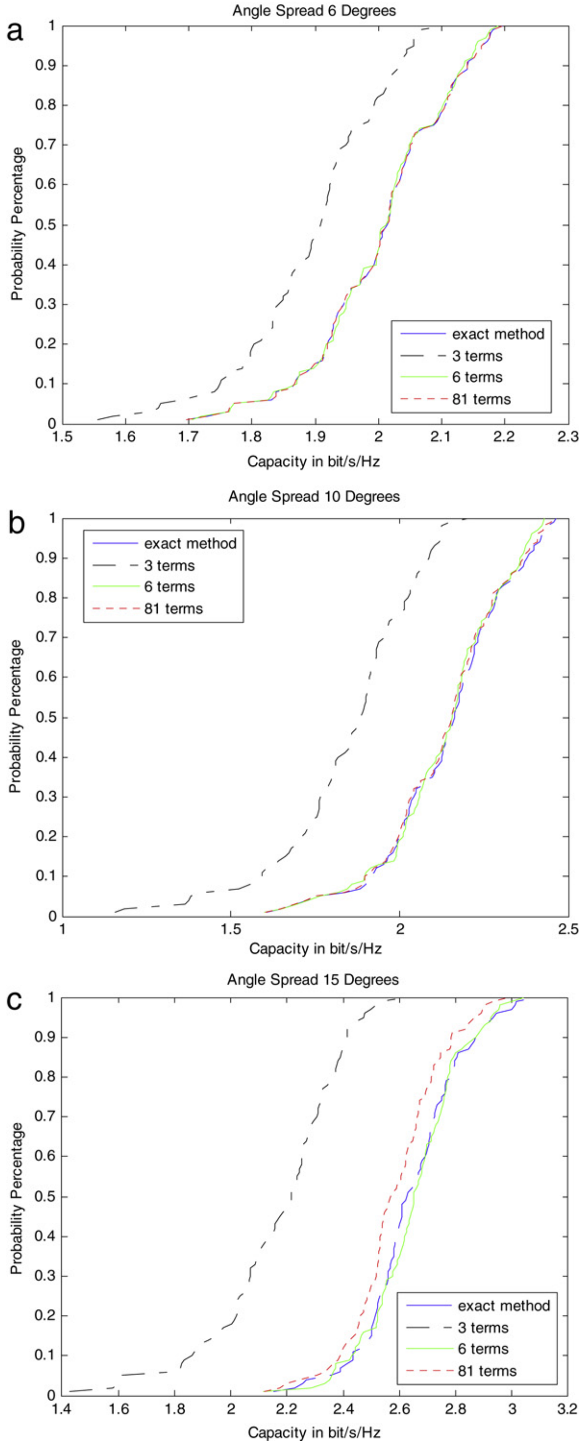

Fig. 4. Comparison of the CDFs of the capacity predicted by the exact method and the approximation method.

4.3. *Evaluation of the approximation method by the extended correlation matrix distance metric*

Based on the validation of the approximation method for the wideband MIMO channels with time-invariant AoAs, we evaluate the validity, reliability and accuracy of the proposed method in (12) by the extended CMD metric. The extended CMD metric presented in [8] can be used to compare the time variation of wideband MIMO channels predicted by the approximation method and the exact method. The definition of the extended CMD is as follows:

$$
d = \frac{\sum_{i=1}^{n_f} d_i}{n_f} = \frac{\sum_{i=1}^{n_f}\left[1 - \frac{\mathrm{tr}\{\mathbf{R}(t_1,f)\mathbf{R}(t_2,f)\}}{\|\mathbf{R}(t_1,f)\|_2\|\mathbf{R}(t_2,f)\|_2}\right]}{n_f} \qquad (17)
$$

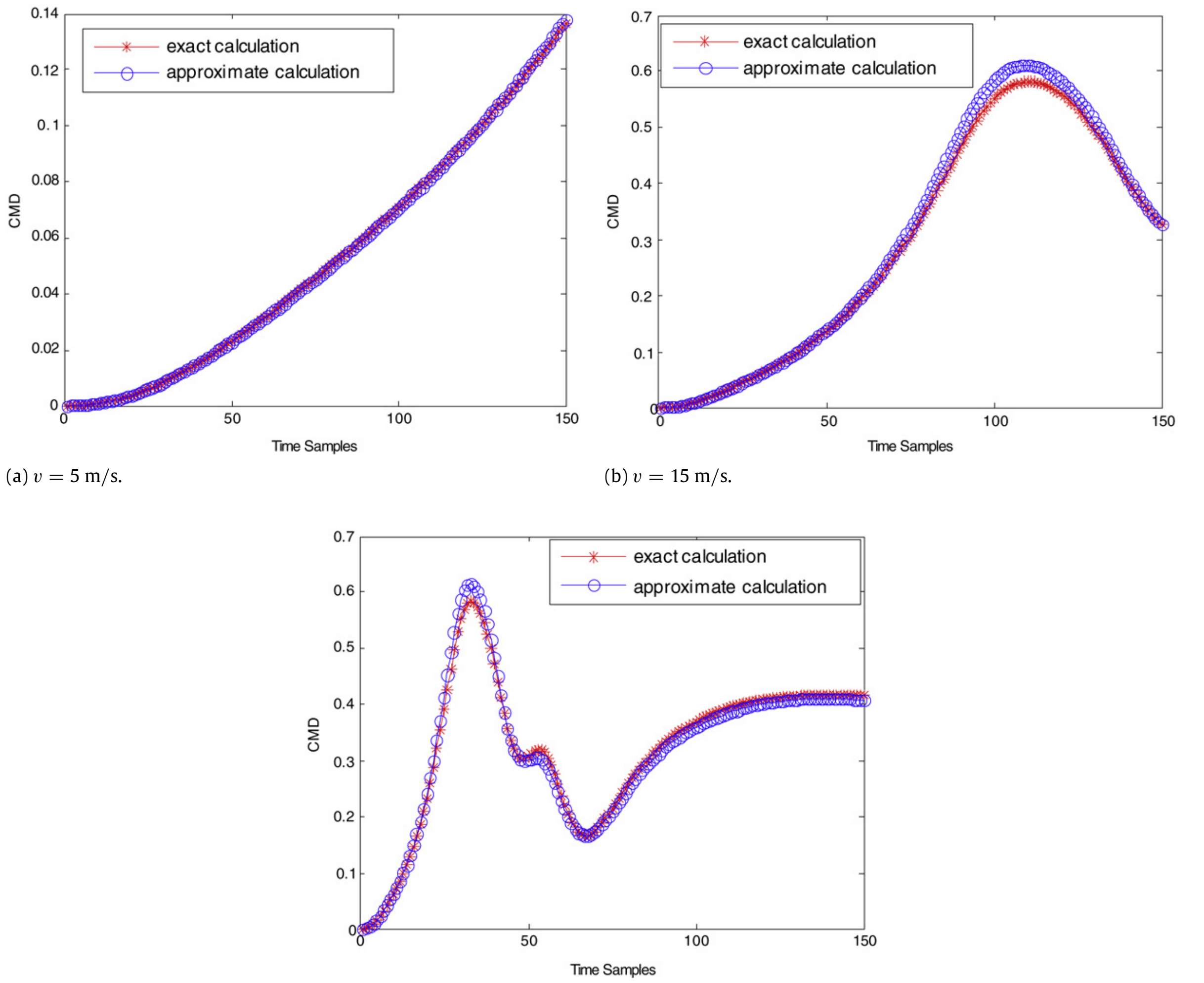

(a) $v = 5$ m/s.

(b) $v = 15$ m/s.

(c) $v = 50$ m/s.

Fig. 5. Comparison of wideband CMDs.

where $\mathbf{R}(t_1, f)$ and $\mathbf{R}(t_2, f)$ are two instantaneous spatial correlation matrices for a certain frequency f given by Eqs. (18) and (19), n_f is the total number of frequencies, the CMD for the wideband channels at each time instant is the averaged value over all the CMDs at all the frequencies.

$$\mathbf{R}(t, f) = \overline{\mathrm{vec}(\mathrm{T}(t, f))\mathrm{vec}(T(t, f))^{\mathrm{H}}} \tag{18}$$

$$\mathbf{T}(t, f) \xleftarrow{\text{Fourier Transformation}} \mathbf{H}(t, \tau_n). \tag{19}$$

Again in (18), the expectation is taken over an ensemble of multi-path phases. Based on this definition, if the instantaneous correlation matrices are identical for all the frequencies, the CMD is zero; while if they vary radically, it will tend to unity.

Comparisons of the CMDs predicted by the approximation method and the exact method have been carried out in various time-variant scenarios at different *Rx* velocities. The simulation results are shown in Fig. 5 for velocity 5 m/s, 15 m/s and 50 m/s, respectively. In all cases the interval between time samples is 30 ms, and the ASs of the clusters are 10°. From these simulation results, we find that the approximation method can provide an estimate of the wideband CMDs very close to those given by the exact model. Although there is a small difference in some cases, the computational complexity has been greatly reduced.

5. Conclusions

In this paper, we have presented a reduced-complexity cluster modeling method to efficiently and effectively approximate the calculations of the spatial correlation matrix and channel matrix for time-variant wideband MIMO channels. The key assumptions made for this approximation method include:

- ULA is used at both the *Tx* and *Rx* sides (or polarized ULA);
- Phases of the MPCs within a cluster are independently draw from a uniform distribution on 0°–360°;
- Moderate angle spread of a cluster (i.e. 10°, according to the evaluation by the extended CMD metric);

- Constant uniform distribution of the angle offsets of MPCs within a cluster.

By evaluating the approximation method with the MSE metric, capacity metric and extended CMD metric, we conclude that the proposed method can provide a simplified simulation of time-variant wideband clustered MIMO channels, requiring the tracking only of cluster centre angles.

Appendix A

1. Determine the last bounce distances (LBDs) of the MPCs at time t_1:

$$lbd_{n,m}(t_1) = \sqrt{lbd_n^2(t_0) + (vt_1)^2 - 2lbd_n(t_0)\, vt_1 \cos\left(\theta_V - \theta_{n,m,AoA}(t_0)\right)}$$

2. Determine the parameter γ using the trigonometric functions:

$$\gamma = \arccos\left(\frac{vt_1 - lbd_n(t_0)\cos\left(\theta_V - \theta_{n,m,AoA}(t_0)\right)}{lbd_{n,m}(t_1)}\right)$$

3. Determine $\theta_{n,m,AoA}(t_1)$: $\theta_{n,m,AoA}(t_1) = \gamma - (\pi - \theta_V)$.

Appendix B

$$\alpha_{1,a}\left(\theta_{R,0}\right) = 2j\pi \cos\left(\theta_{R,0}\right) a$$
$$\alpha_{2,a}\left(\theta_{R,0}\right) = -\left(2\pi^2 \cos^2\left(\theta_{R,0}\right) a^2 + j\pi \sin\left(\theta_{R,0}\right) a\right).$$

References

[1] D. Shiu, G.J. Foschini, M.J. Gans, J.M. Kahn, Fading correlation and its effect on the capacity of multielement antenna systems, IEEE Transactions on Communications 48 (March) (2000) 502–513.

[2] K. Li, M. Ingram, A. Van Nguyen, Impact of clustering in statistical indoor propagation models on link capacity, IEEE Transactions on Communications 50 (4) (2002) 521–523.

[3] H. Xiao, A.G. Burr, L. Song, A time-variant wideband spatial channel model based on the 3GPP model, in: VTC-Fall 2006, Montreal, Canada, September 2006.

[4] 3GPP TR 25.996 V6.1.0 (2003–09), Technical Report. Available www.3gpp.org.

[5] A. Molisch, Modeling the MIMO propagation channel, Belgian Journal of Electronics and Communications 4 (2003) 5–14.

[6] H. Asplund, A.F. Molisch, M. Steinbauer, N.B. Mehta, Clustering of the scatterers in mobile radio channels — evaluation and modeling in the COST259 directional channel model, in: IEEE International Conference on Communications, 2002.

[7] Hui Xiao, Alister G. Burr, Rodrigo C. de Lamare, Reduced-complexity cluster modeling for the 3GPP channel model, in: IEEE International Conference on Communications, ICC 2007, Glasgow, Scotland, 24–28 June, 2007.

[8] Hui Xiao, Alister G. Burr, An extended correlation matrix distance metric used to evaluate the short-term time variation of wideband channels predicted by different MIMO channel models, in: NEWCOM-ACoRN Joint Workshop 2006, Vienna, Austria.

[9] Alister G. Burr, On the channel autocorrelation matrix of a MIMO system, in: COST 273 TD(04)108, Sweden 7–10 Jan. 2004.

[10] Eric W. Weisstein, Taylor Series, From Mathworld — A Wolfram Web Resource. http://mathworld.wolfram.com/TaylorSeries.html.

[11] A Web Resource. http://www.maplesoft.com.

[12] I.E. Telatar, Capacity of multi-antenna Gaussian channels, European Transactions on Telecommunications 10 (6) (1999) 585–595.

[13] G.J. Foschini, M.J. Gans, On limits of wireless communications in a fading environment when using multiple antennas, Wireless Personal Communications 6 (3) (1998) 311–335.

[14] P.W. Wolniansky, G.J. Foschini, G.D. Golden, R.A. Valenzuela, V-BLAST: An architecture for realizing very high data rates over the rich-scattering wireless channel, in: 1998 URSI International Symposium on Signals, Systems and Electronics, ISSSE 98, 1998, pp. 295–300.

[15] I. Miller, M. Miller, John E. Freund's Mathematical Statistics with Applications, seventh edition, Pearson Prentice Hall, Pearson Education, Inc., Upper Saddle River, NJ 07458, p. 325.

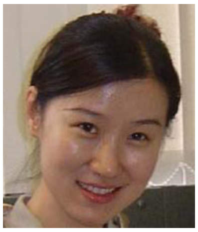

Hui Xiao received the B.Eng degree in Mechanical and Electrical Engineering from the Beijing Institute of Technology, China, in 2004, and the Ph.D. degree in Electronics Engineering from the University of York, UK, in 2008.

Her main research interests include wireless communications, MIMO technology, channel modeling, OFDM, digital signal processing.

Alister G. Burr received a B.Sc. degree from the University of Southampton, UK in 1979, and Ph.D. from the University of Bristol in 1984. He was at Thorn-EMI Central Research Laboratories from 1979 until 1985, and since 1985 has been with Dept. of Electronics, University of York, UK, since 2001 as Professor of Communications. In 1999 he was Visiting Professor at Vienna University of Technology, and in 2000–2001 he held a Royal Society Senior Research Fellowship. He is currently Chair of Working Group 1 in the European COST Action 2100, on mobile and wireless communications, and a member of the editorial board of PHYCOM. His research interests are in modulation and coding for wireless communications, and especially turbo-codes and turbo-processing, MIMO systems and MIMO channel modeling, and cooperative relaying.